

# Hagen-Poiseuille and thermal transpiration flows of a highly rarefied gas

Hitoshi Funagane<sup>1</sup> and Shigeru Takata<sup>1,2</sup>

<sup>1</sup>Department of Mechanical Engineering and Science, Kyoto University, Kyoto 606-8501, Japan

<sup>2</sup>Advanced Research Institute of Fluid Science and Engineering, Kyoto University, Kyoto 606-8501, Japan

## Abstract

Hagen-Poiseuille and thermal transpiration flows of a highly rarefied gas through a long circular pipe are investigated on the basis of the linearized Boltzmann equation for hard-sphere molecules with the diffuse reflection condition. The net mass flows of the both problems in the highly rarefied regime are obtained by an iterative approximation method with an explicit convergence estimate. The singular behavior of the velocity distribution functions in that regime is also clarified.

## 1 Introduction

A flow induced by a pressure gradient (Poiseuille flow) and a flow induced by a temperature gradient (thermal transpiration, see, e.g., Ref. [9]) are classical and fundamental problems of rarefied gas dynamics, and have been extensively studied by many researchers (see, e.g., Refs. [1, 3, 5–9] and the references therein).

In the present study, we shall focus on Hagen-Poiseuille and thermal transpiration flows of a highly rarefied gas through a circular pipe, for the purpose of obtaining the accurate data of the net mass flows. In the highly rarefied regime, an accurate analysis of these flows on the basis of the (linearized) Boltzmann equation is a hard task because of the singular behavior of the velocity distribution functions, in addition to the complex collision operator of the equation. In order to overcome these difficulties, we use an iterative approximation method with an explicit convergence estimate, which was recently developed by the authors in Ref. [11] with the aid of the mathematical estimates given by Chen *et al.* [2]. Main advantage of this method is that we can start the iterative process from an initial guess with an explicit form that contains the majority of the singularity in the velocity distribution functions. Moreover, the method gives an estimate on the required number of iterations to obtain the practical converged solution and the behavior of the velocity distribution function at each stage of iteration.

The paper is organized as follows. In section 2, we formulate the problems. In section 3, we present an iterative approximation method and its explicit convergence estimate at each stage of iteration in the highly rarefied regime. Also, we clarify the behavior of the velocity distribution functions by using the estimate. In section 4, we present the numerical methods based on the iterative approximation method. Numerical results are shown in section 5.

## 2 Problem and formulation

Consider a highly rarefied gas in a long pipe with a uniform circular cross section. Let the radius of the pipe be  $D$  and the  $X_3$  axis be parallel to the pipe. The pressure of the gas is given by  $p_0(1 + c_P X_3/D)$  and the temperature of the pipe wall is given by  $T_0(1 + c_T X_3/D)$  ( $c_P$  and  $c_T$  are constants). We investigate the steady gas flows under the following assumptions: (i) the behavior of the gas is described by the Boltzmann equation for hard-sphere molecules (the mass of a molecule is  $m$  and the diameter of a molecule is  $d_m$ ); (ii) the gas molecules are diffusely reflected on the surface of the pipe; and (iii)  $|c_P|$ ,  $|c_T| \ll 1$ , so that the equation and the boundary condition can be linearized around the equilibrium state at rest with the pressure  $p_0$  and the temperature  $T_0$ .

Let us denote the molecular velocity by  $(2RT_0)^{1/2}\zeta_i$  and the velocity distribution function of the gas molecules by  $\rho_0(2RT_0)^{-3/2}[E^{1/2} + \phi(x_i, \zeta_i)]E^{1/2}$ , where  $x_i = X_i/D$ ,  $\rho_0 = p_0/RT_0$ ,  $R$  is the specific gas constant,  $\zeta = (\zeta_i^2)^{1/2}$ , and  $E = \pi^{-3/2} \exp(-\zeta^2)$ . Let us denote the density of the gas by  $\rho_0(1 + \sigma)$ , the flow velocity by  $(2RT_0)^{1/2}u_i$ , the temperature by  $T_0(1 + \tau)$ , the pressure by  $p_0(1 + P)$ , the stress tensor by  $p_0(\delta_{ij} + P_{ij})$ , and the heat-flow vector by  $p_0(2RT_0)^{1/2}Q_i$ , where  $\delta_{ij}$  is Kronecker's delta. Then, the problem is described by the following-boundary value problem for  $\phi$ :

$$\zeta_i \frac{\partial \phi}{\partial x_i} = -\frac{\nu(\zeta)}{k} \phi + \frac{1}{k} K(\phi), \quad (1)$$

$$\phi = c_T(\zeta^2 - 2)E^{1/2}x_3 - 2\sqrt{\pi}E^{1/2} \int_{\zeta_i n_i < 0} \zeta_i n_i \phi E^{1/2} d\zeta \quad \text{for } \zeta_i n_i > 0, \quad x_1^2 + x_2^2 = 1, \quad (2)$$

where  $(2/3) \int \zeta^2 \phi E^{1/2} d\zeta = c_P x_3$  and with

$$K(\phi) = \int \kappa(\zeta_{i*}, \zeta_i) \phi(x_i, \zeta_{i*}) d\zeta_{i*}, \quad (3)$$

$$\begin{aligned} \kappa(\zeta_{i*}, \zeta_i) = & \frac{1}{\sqrt{2\pi}} \frac{1}{|\zeta_i - \zeta_{i*}|} \exp\left(-\frac{(|\zeta_{i*}|^2 - |\zeta_i|^2)^2}{4|\zeta_{i*} - \zeta_i|^2} - \frac{|\zeta_{i*} - \zeta_i|^2}{4}\right) \\ & - \frac{1}{2\sqrt{2\pi}} |\zeta_i - \zeta_{i*}| \exp\left(-\frac{|\zeta_{i*}|^2 + |\zeta_i|^2}{2}\right), \end{aligned} \quad (4)$$

$$\nu(\zeta) = \frac{1}{2\sqrt{2}} \left[ \exp(-\zeta^2) + \left(2\zeta + \frac{1}{\zeta}\right) \int_0^\zeta \exp(-s^2) ds \right], \quad (5)$$

$$k = \frac{\sqrt{\pi} l_0}{2 D}, \quad l_0 = \frac{1}{\sqrt{2\pi} d_m^2 (\rho_0/m)}. \quad (6)$$

Here,  $n_i$  is the unit normal vector to the boundary, pointed to the gas and  $l_0$  is the mean free path of the gas molecules in the equilibrium state at rest. Note that we shall use  $k$  in place of the Knudsen number  $\text{Kn} (= l_0/D)$  to indicate the degree of gas rarefaction.

Let us introduce the cylindrical coordinate system  $(r, \theta, x_3)$  and  $(\eta, \alpha, w)$  in position and molecular velocity spaces:  $x_1 = r \cos \theta$ ,  $x_2 = r \sin \theta$ ,  $\zeta_1 = \eta \cos(\theta + \alpha)$ ,  $\zeta_2 = \eta \sin(\theta + \alpha)$ ,  $\zeta_3 = w$  (see figure 1).  $\eta$  is the absolute value of the molecular velocity in  $\zeta_1$ - $\zeta_2$  plane. Assuming the axisymmetry about the  $x_3$ -axis, we can seek  $\phi$  in the form of

$$\phi = c_P[Fx_3 + \phi_P(r, \eta, \alpha, w)] + c_T[(\eta^2 + w^2 - 5/2)Fx_3 + \phi_T(r, \eta, \alpha, w)], \quad (7)$$

$$F = \pi^{-3/4} \exp\left(-\frac{\eta^2 + w^2}{2}\right), \quad (8)$$

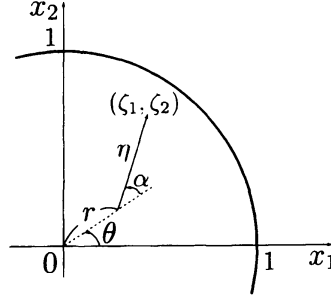


Fig. 1: Cylindrical coordinate system.

where  $\phi_J$  ( $J = P$  or  $T$ ) is the solution of the following boundary-value problem:

$$\eta \cos \alpha \frac{\partial \phi_J}{\partial r} - \frac{\eta \sin \alpha}{r} \frac{\partial \phi_J}{\partial \alpha} = -\frac{\nu}{k} \phi_J + \frac{1}{k} K(\phi_J) - I_J, \quad (9)$$

$$\phi_J = 0 \quad \text{for } \cos \alpha < 0, \quad r = 1, \quad (10)$$

$$I_P = wF, \quad I_T = w(\eta^2 + w^2 - 5/2)F. \quad (11)$$

Physically,  $\phi_P$  represents the solution of the Hagen-Poiseuille flow, while  $\phi_T$  represents that of the thermal transpiration. Here we have also assumed that  $\phi_J$  is odd in  $w$  and symmetric in  $\alpha$  in the following sense:

$$\phi_J(r, \eta, \alpha, w) = \phi_J(r, \eta, 2\pi - \alpha, w). \quad (12)$$

The macroscopic variables are expressed as

$$\begin{aligned} \sigma &= (c_P - c_T)x_3, & \tau &= c_T x_3, & P &= c_P x_3, \\ u_1 &= u_2 = 0, & u_3 &= c_P u[\phi_P] + c_T u[\phi_T], \\ Q_1 &= Q_2 = 0, & Q_3 &= c_P Q[\phi_P] + c_T Q[\phi_T], \\ P_{11} &= P_{22} = P_{33} = c_P x_3, & P_{12} &= 0, & P_{23} &= -\frac{r}{2} c_P \sin \theta, & P_{31} &= -\frac{r}{2} c_P \cos \theta, \end{aligned} \quad (13)$$

where

$$u[f] = 4 \int_0^\infty \int_0^\pi \int_0^\infty \eta w f F d w d \alpha d \eta, \quad (14)$$

$$Q[f] = 4 \int_0^\infty \int_0^\pi \int_0^\infty \eta w \left( \eta^2 + w^2 - \frac{5}{2} \right) f F d w d \alpha d \eta. \quad (15)$$

Note that the density, temperature and pressure of the gas are uniform in each cross-section and linearly depend on  $x_3$ . The net mass flow through the pipe, which we denote by  $\rho_0(2RT_0)^{1/2}\pi D^2 \mathcal{M}$ , is written by

$$\mathcal{M} = c_P M[\phi_P] + c_T M[\phi_T], \quad M[f] = 2 \int_0^1 u[f] r dr. \quad (16)$$

### 3 Iterative approximation method

Integrating Eq. (9) along its characteristic line with the boundary condition (10), we obtain the following expression for  $\phi_J$ :

$$\phi_J = \phi_J^{(0)} + \int_0^{d_B} \frac{1}{k\eta} e^{-\frac{\nu}{k\eta}s} K(\phi_J)_{(\tilde{r}, \eta, \tilde{\alpha}, w)} ds, \quad (17)$$

$$\phi_J^{(0)} = -\frac{k}{\nu} \left[ 1 - \exp\left(-\frac{\nu}{k\eta} d_B\right) \right] I_J, \quad (18)$$

with

$$d_B = r \cos \alpha + \sqrt{1 - r^2 \sin^2 \alpha}, \quad (19a)$$

$$\tilde{r} = \sqrt{r^2 - 2rs \cos \alpha + s^2}, \quad (19b)$$

$$\tilde{\alpha} = \cos^{-1} \left( \frac{r \cos \alpha - s}{\sqrt{r^2 - 2rs \cos \alpha + s^2}} \right). \quad (19c)$$

Here,  $d_B$  is the distance from  $x_i$  to the point on the boundary in the direction of  $(-\zeta_1, -\zeta_2, 0)$ . Note that, in Eq. (17),  $K(\phi_J)$  is a function of  $\tilde{r}$  and  $\tilde{\alpha}$  dependent on  $s$ .

We consider a sequence of functions  $\phi_J^{(0)}, \phi_J^{(1)}, \phi_J^{(2)}, \dots$  generated by the following iterative process:

$$\phi_J^{(n)} = \phi_J^{(0)} + \int_0^{d_B} \frac{1}{k\eta} e^{-\frac{\nu}{k\eta}s} K(\phi_J^{(n-1)})_{(\tilde{r}, \eta, \tilde{\alpha}, w)} ds \quad n = 0, 1, 2, \dots, \quad (20)$$

with  $\phi_J^{(-1)} = 0$ . By using the mathematical estimates given by Chen *et al.* [2], we can prove the following for  $k \gg 1$ :

(a)  $\{\phi_J^{(n)}\}$  is a Cauchy sequence in  $L^\infty$ , where the norm is defined by  $\|f\|_\infty = \sup_{C_i} |f|$  for each  $x_i$ . The limiting function of  $\phi_J^{(n)}$  is the solution  $\phi_J$ :  $\phi_J = \lim_{n \rightarrow \infty} \phi_J^{(n)}$  ( $J = P$  or  $T$ ).

(b) By introducing the sequence of functions  $\{\psi_J^{(n)}\}$ , defined by  $\psi_J^{(n)} = \phi_J^{(n)} - \phi_J^{(n-1)}$  ( $n \geq 1$ ) and  $\psi_J^{(0)} = \phi_J^{(0)}$ ,  $\phi_J^{(n)}$  is rewritten as  $\phi_J^{(n)} = \sum_{i=0}^n \psi_J^{(i)}$ . Thus  $\phi_J$  can be obtained as the sum of  $\psi_J^{(n)}$ :  $\phi_J = \sum_{i=0}^{\infty} \psi_J^{(i)}$  ( $J = P$  or  $T$ ).  $\psi_J^{(n)}$  is generated by the following iterative process:

$$\psi_J^{(n)} = \int_0^{d_B} \frac{1}{k\eta} e^{-\frac{\nu}{k\eta}s} K(\psi_J^{(n-1)})_{(\tilde{r}, \eta, \tilde{\alpha}, w)} ds \quad n = 1, 2, \dots \quad (21)$$

There are positive constants  $C_0$  and  $C_1$  independent of  $k$  such that, for  $i = 0, 1, \dots$ ,

$$|\psi_J^{(i)}| \leq C_0(\eta + k^{-1})^{-1} [C_1 k^{-1} (\ln k + 1)]^i, \quad (22a)$$

$$|K(\psi_J^{(i)})| \leq C_0(1 + \ln k) [C_1 k^{-1} (\ln k + 1)]^i, \quad (22b)$$

$$|M[\psi_J^{(i)}]| \leq C_0 [C_1 k^{-1} (\ln k + 1)]^i. \quad (22c)$$

On the one hand, estimate (22c) shows that the net mass flow at each stage of iteration will be decreased with the rate  $O(k^{-1}(\ln k + 1))$ . As  $k$  is increased, the rate will be decreased. Therefore, in the highly rarefied regime, the converged solution will be

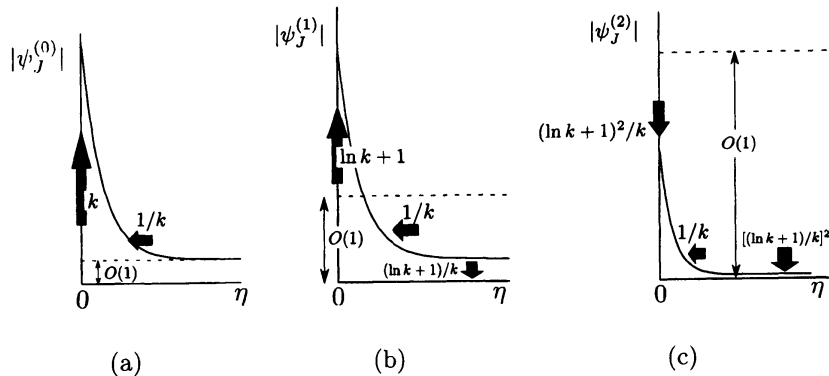


Fig. 2: Change of  $\psi_J^{(0)}$ ,  $\psi_J^{(1)}$ ,  $\psi_J^{(2)}$  as  $k$  is increased ( $k \gg 1$ ). (a)  $\psi_J^{(0)}$ , (b)  $\psi_J^{(1)}$ , (c)  $\psi_J^{(2)}$ . The rate and direction of change when  $k$  is increased are shown.

obtained within several iterations. [Actually, we needed six iterations for  $k = 10$  and less iterations for  $k > 10$  (see section 5.2).] On the other hand, estimate (22a) presents that the velocity distribution function at each stage of iteration will be scaled down with the rate  $O(k^{-1}(\ln k + 1))$ . We show the feature for  $i = 0, 1, 2$  schematically in figure 2. The figure shows that  $\psi_J^{(0)}$  will be changed from  $O(k)$  to  $O(1)$ , and  $\psi_J^{(1)}$  will be changed from  $O(\ln k)$  to  $O(1)$  in the range of  $O(k^{-1})$  in  $\eta$ . In other words,  $\psi_J^{(0)}$  and  $\psi_J^{(1)}$  grow locally near  $\eta = 0$  as  $k$  is increased. In order to carry out accurate numerical computations for large  $k$ , a special attention should be paid to capture the singular behavior of the velocity distribution functions.

## 4 Numerical method

The net mass flow at the initial guess  $M[\psi_J^{(0)}]$ , obtained by substituting  $\psi_J^{(0)}$  into Eq. (16), is expressed as the forthfold integral. This integral is easily numerically carried out by first applying the double exponential (DE) transformation [12] to all integration variables and using the trapezoidal formula for the transformed variables. The number of lattice points used in this computation is 49 for  $r$ , 65 for  $\eta$ , 130 for  $\alpha$  and 97 for  $w$  in the ranges of  $0 < r < 1$ ,  $0 < \eta < 4.39$ ,  $0 < \alpha < \pi$  and  $0 < w < 5.93$ .

As the first step to obtain higher order corrections  $\psi_J^{(n)}$  ( $n \geq 1$ ), by making use of the iterative process (21), we seek  $K(\psi_J^{(n-1)})$ . In the computation, there are two things that should be paid attention to. One is the fact that  $\psi_J^{(0)}$  and  $\psi_J^{(1)}$  behave steeply near  $\eta = 0$ , as seen from estimate (22a). The other is the singularity  $|\zeta_i - \zeta_{i*}|^{-1}$  in Eq. (4). In order to overcome these difficulties, we first make the variable transformation from  $(\eta_*, \alpha_*, w_*)$  to  $(P, \beta, w_*)$  to manage the singularity  $|\zeta_i - \zeta_{i*}|^{-1}$  (see Appendix A). Due to the variable transformation, in the computation of  $\tilde{L}_1$ , we have to capture the singular behavior of the velocity distribution function on the transformed coordinate system  $(P, \beta, w_*)$ . From the definition of  $\eta_*$  [see Eq. (33)], we find that  $\eta_* = 0$  corresponds to  $P = 0$ ,  $P = \eta$ ,  $\beta = 0$ ,  $\beta = \pi$  and  $\beta = 2\pi$  on the transformed system for arbitrary  $\eta$ . Taking into account this information, we divide the domain of the integration in such a way that  $0 < P < \eta$  and  $\eta < P$  for  $P$ ,  $0 < \beta < \pi$  and  $\pi < \beta < 2\pi$  for  $\beta$ . Thus, the velocity distribution

function will be localized near the end points of the domains of integrations. The DE transformation with the trapezoidal formula is an efficient numerical integration method for an integrand with an end-point singularity. By using the DE transformation, we can numerically handle the singular behavior of the velocity distribution function in  $\tilde{L}_1$  and  $\tilde{L}_2$  without difficulties. For  $\tilde{L}_2$ , we do not need to divide the domain of the integration because the velocity distribution function is already localized near the end-point ( $\eta_* = 0$ ). In the computation of  $\tilde{L}_1$ , we give an additional care in the case of  $r = 1$ , because  $\psi_J^{(n-1)}$  has discontinuity at  $\alpha = \pi/2$  (for example, see (c) and (f) of figure 3). As to the integration with respect to  $s$  in Eq. (21), we first interpolate  $K(\psi_J^{(n-1)})$  for  $\tilde{r}$  and  $\tilde{\alpha}$  [see Eqs. (19b) and (19c)] because the obtained  $K(\psi_J^{(n-1)})$  is a function of  $r$ ,  $\eta$ ,  $\alpha$  and  $w$ . After the interpolation,  $K(\psi_J^{(n-1)})$  can be approximated by the piecewise quadratic function on the lattice points of  $s$ . Thus, the integral of the approximated  $K(\psi_J^{(n-1)})$  multiplied by  $\exp(-\nu s/k\eta)$  is carried out analytically. We numerically calculate  $M[\psi_J^{(n)}]$  expressed as the forthfold integral. The integration with respect to  $r$  is carried out by using the Simpson formula, and the integrations with respect to  $\eta$ ,  $\alpha$  and  $w$  are performed by the trapezoidal formula after the DE transformation.

## 5 Numerical results

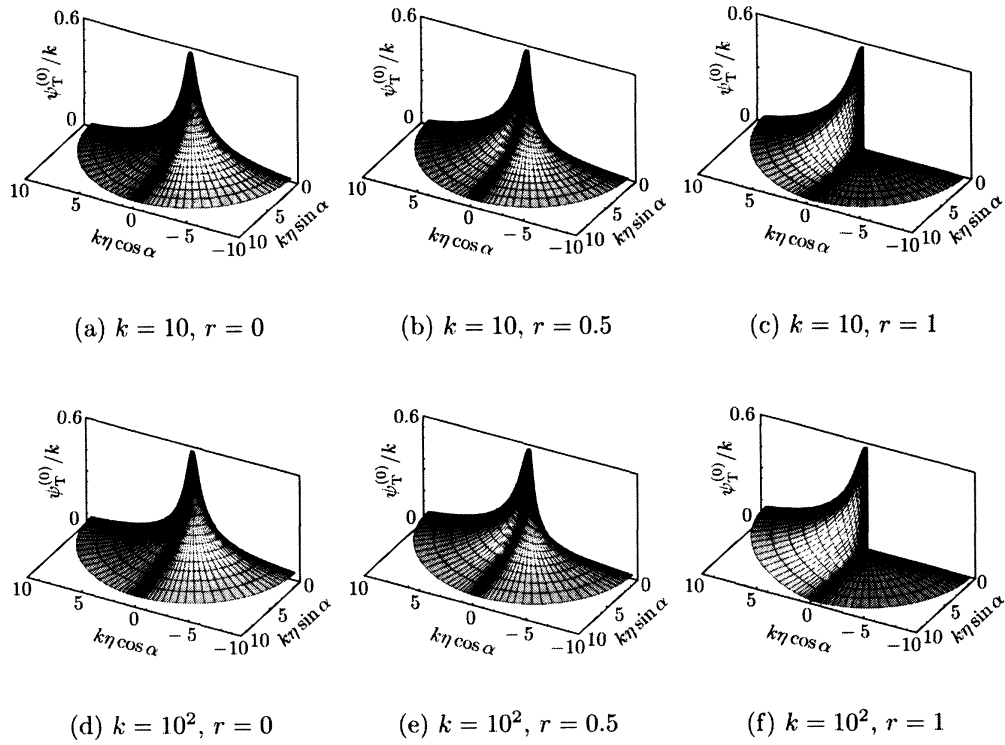
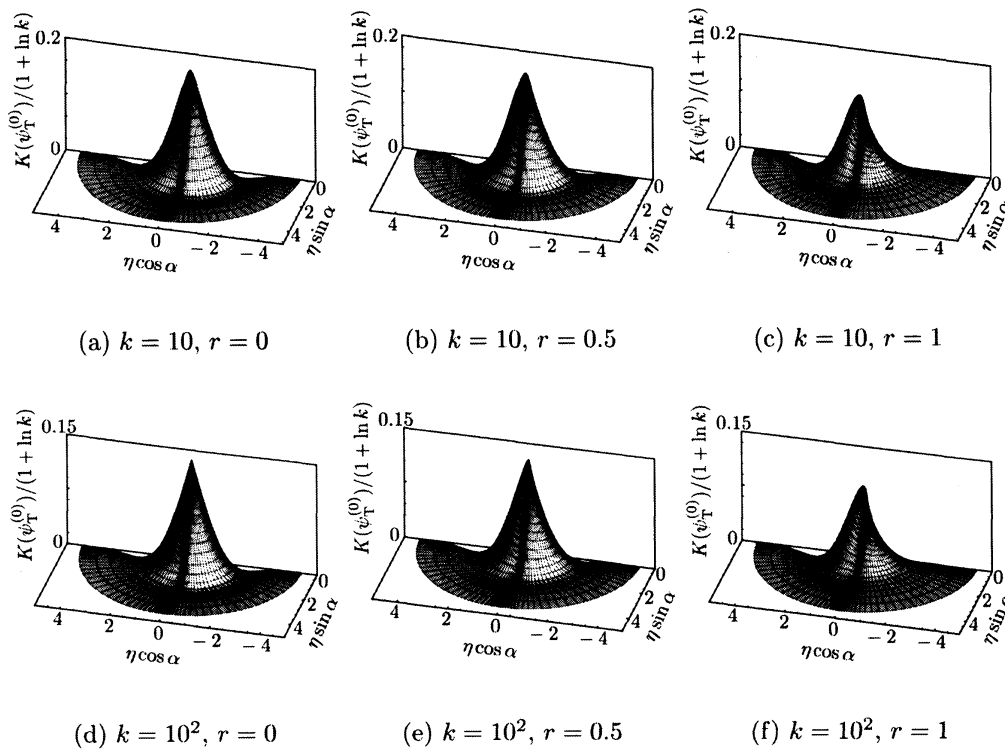
In our computation, the molecular velocity space is limited to  $0 < \eta < 4.39$ ,  $0 < w < 5.93$ . The number of lattice points used in the computation of higher order corrections is 21 for  $r$ , 65 for  $\eta$ , 130 for  $\alpha$  ( $0 < \alpha < \pi$ ) and 97 for  $w$ .

### 5.1 Velocity distribution functions

The initial guess  $\psi_T^{(0)}$ , the initial collision operator  $K(\psi_T^{(0)})$  and the first correction  $\psi_T^{(1)}$  at three points in the gas region are shown for  $k = 10$  and  $10^2$  in figures 3–5. On the one hand,  $\psi_T^{(0)}$  is  $O(k)$  and  $\psi_T^{(1)}$  is  $O(\ln k + 1)$ . Both of them are localized in the region of  $\eta \leq k^{-1}$ . On the other hand,  $K(\psi_T^{(0)})$ , which is  $O(\ln k + 1)$ , behaves moderately in  $\eta$ . In other words, the trace of the singular behavior of  $\psi_T^{(0)}$  is disappeared in  $K(\psi_T^{(0)})$ . That is, the singular behavior of  $\psi_T^{(0)}$  is disappeared by the action of the collision operator with scaling down by the factor  $O(k^{-1}(\ln k + 1))$ . By the action of the integration in Eq. (21), a singular distribution is reproduced in  $\psi_T^{(1)}$  with the scale unchanged. We can observe the process of disappearance and reproduction of singular velocity distributions in the longer transition from  $\psi_T^{(0)}$  to  $\psi_T^{(4)}$  at  $r = 0$  for  $k = 10$  in figure 6. Estimates (22a)–(22c) may not be optimal, but the numerical results shown in figures 3–6 support that the estimates are actually optimal.

### 5.2 Net mass flows

We have obtained the net mass flows of the both problems for several values of  $k$ . The numerical results of the initial guess  $M[\phi_J^{(0)}]$ , the first correction  $M[\phi_J^{(1)}]$  and the converged solution  $M[\phi_J^{(n)}]$  are shown in table 1. Here  $\phi_J^{(n)} = \sum_{i=0}^n \psi_J^{(i)}$  ( $J = P$  or  $T$ ). The value of  $M[\phi_J^{(n)}]$  is converged to 4 digits.  $M[\phi_J^{(n)}]$  versus  $k$  is shown in figure 7.

Fig. 3:  $\psi_T^{(0)}$  at  $w = 0.633$ .Fig. 4:  $K(\psi_T^{(0)})$  at  $w = 0.633$ .

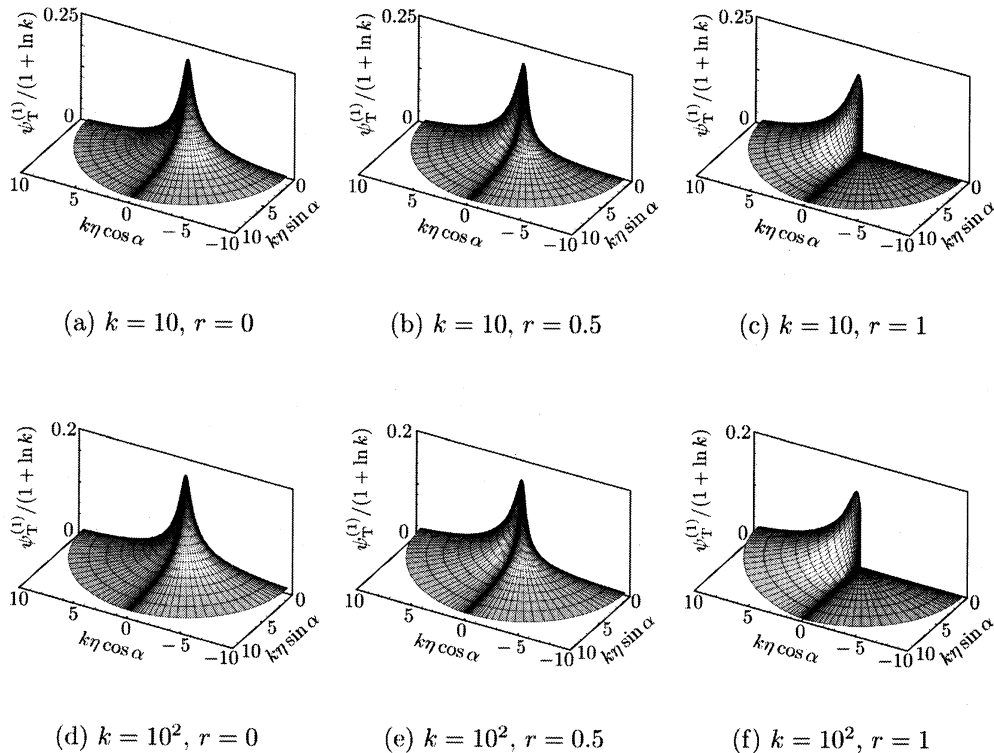


Fig. 5:  $\psi_T^{(1)}$  at  $w = 0.633$ .

Finally, we list some data that show the accuracy of our computation as follows:

- (i) We have limited the molecular velocity space to a finite region. In the computation,  $|\phi_J^{(n)} F|$  is less than  $3.0 \times 10^{-9}$  outside the region.
- (ii) The collision integral  $K(\phi) - \nu\phi$  for the Maxwellian  $\phi = F$ , which should theoretically be zero, is bounded by  $5.0 \times 10^{-7}$ .  $\nu F$  is of the order of 0.3.
- (iii) The following moment, which should theoretically be zero, is bounded by

$$\left| \int_0^\infty \int_0^\pi \int_0^\infty \eta w [K(\phi_J) - \nu\phi_J] F d w d \alpha d \eta \right| \leq 5.0 \times 10^{-6}. \quad (23)$$

## 6 Conclusion

We have investigated Hagen-Poiseuille and thermal transpiration flows of a highly rarefied gas through a circular pipe for purpose of obtaining the accurate net mass flows. In the present work, motivated by the previous work by the authors, we have applied an iterative approximation method with an explicit convergence estimate to the problems, and have clarified the singular behavior of the velocity distribution function. By making use of the method, with a special attention to the singular behavior of the velocity distribution function, we have also obtained the net mass flows for several values of  $k$ .

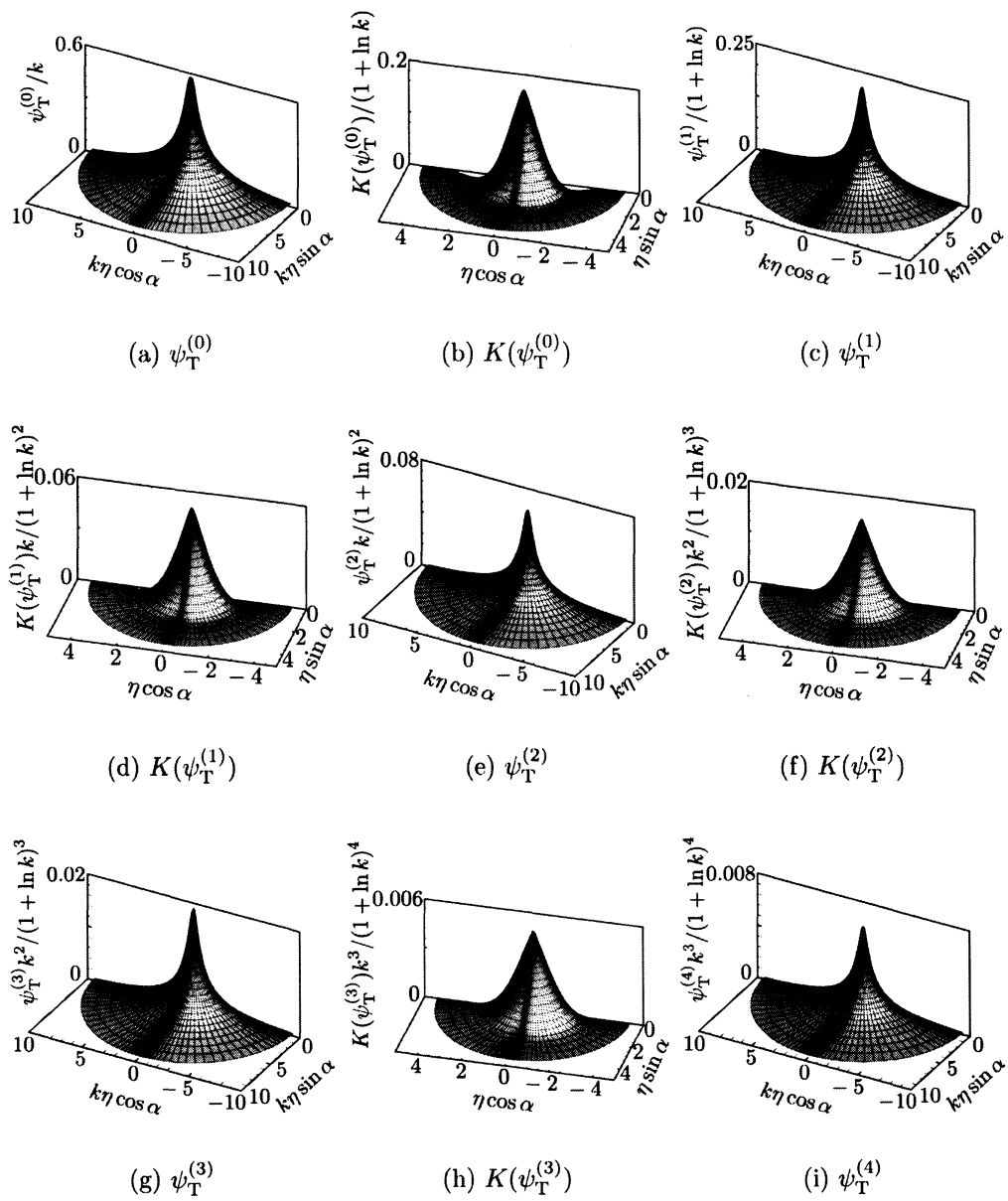


Fig. 6: Transition from  $\psi_T^{(0)}$  to  $\psi_T^{(4)}$  at  $r = 0$  and  $w = 0.633$  for  $k = 10$ .

Table 1: Net mass flows in the highly rarefied regime.

	$M[\phi_T^{(0)}]$	$M[\phi_T^{(1)}]$	$M[\phi_T^{(n)}]$
$k = 10$	0.2833	0.3191	0.3244 <sup>(6*)</sup>
$k = 10^2$	0.3585	0.3642	0.3643 <sup>(3)</sup>
$k = 10^3$	0.3735	0.3741	0.3741 <sup>(2)</sup>
$k = 10^4$	0.3758	0.3758	0.3758 <sup>(1)</sup>
$k = 10^5$	0.3761	–	0.3761 <sup>(0)</sup>
$k = 10^6$	0.3761	–	0.3761 <sup>(0)</sup>
	$M[\phi_P^{(0)}]$	$M[\phi_P^{(1)}]$	$M[\phi_P^{(n)}]$
$k = 10$	-0.6113	-0.6915	-0.7037 <sup>(6)</sup>
$k = 10^2$	-0.7269	-0.7385	-0.7387 <sup>(3)</sup>
$k = 10^3$	-0.7486	-0.7498	-0.7498 <sup>(2)</sup>
$k = 10^4$	-0.7518	-0.7519	-0.7519 <sup>(2)</sup>
$k = 10^5$	-0.7522	–	-0.7522 <sup>(0)</sup>
$k = 10^6$	-0.7522	–	-0.7522 <sup>(0)</sup>

\* Converged data. The superscript number indicates the order of approximation  $n$ .

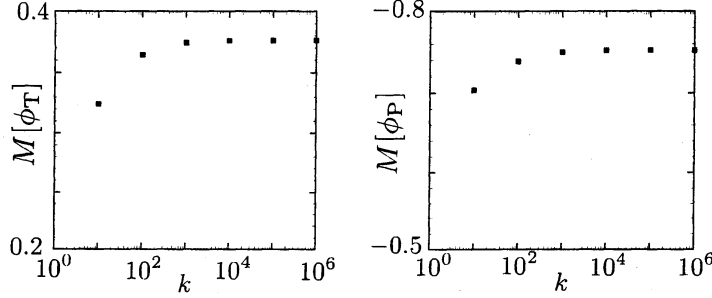


Fig. 7: Net mass flows as a function of  $k$ . Left figure shows  $M[\phi_T]$  versus  $k$  and right figure shows  $M[\phi_P]$  versus  $k$ . ■ indicates the present data.

## Appendix A Collision operator $K$

The collision operator  $K(\phi_J)$  is written in the following form:

$$K(\phi_J) = \tilde{L}_1(\phi_J) - \tilde{L}_2(\phi_J), \quad (24)$$

where

$$\tilde{L}_1(\phi_J) = \int_0^\infty \int_0^{2\pi} \int_{-\infty}^\infty \frac{1}{\sqrt{2\pi}} \frac{\eta_*}{|\zeta_{i*} - \zeta_i|} \exp\left(-\frac{(\eta_*^2 + w_*^2 - \eta^2 - w^2)^2}{4|\zeta_{i*} - \zeta_i|^2} - \frac{|\zeta_{i*} - \zeta_i|^2}{4}\right) \times \phi_J(r, \eta_*, \alpha_*, w_*) dw_* d\alpha_* d\eta_*, \quad (25)$$

$$\tilde{L}_2(\phi_J) = \int_0^\infty \int_0^{2\pi} \int_{-\infty}^\infty \Omega_2(\eta, \alpha, w, \eta_*, \alpha_*, w_*) \phi_J(r, \eta_*, \alpha_*, w_*) dw_* d\alpha_* d\eta_*, \quad (26)$$

$$\Omega_2(\eta, \alpha, w, \eta_*, \alpha_*, w_*) = \frac{\eta_*}{2\sqrt{2\pi}} |\zeta_{i*} - \zeta_i| \exp\left(-\frac{\eta_*^2 + w_*^2 + \eta^2 + w^2}{2}\right), \quad (27)$$

$$|\zeta_{i*} - \zeta_i| = [\eta^2 + w^2 + \eta_*^2 + w_*^2 - 2\eta\eta_* \cos(\alpha_* - \alpha) - 2ww_*]^{1/2}. \quad (28)$$

In order to manage the singularity  $|\zeta_i - \zeta_{i*}|^{-1}$  in  $\tilde{L}_1$ , we make the variable transformation from  $(\eta_*, \alpha_*, w_*)$  to  $(P, \beta, w_*)$  which was used in Ref. [10]:

$$\zeta_{1*} - \zeta_1 = P \cos(\beta + \beta_0), \quad \zeta_{2*} - \zeta_2 = P \sin(\beta + \beta_0), \quad w_* = w_*, \quad (29)$$

where  $\beta_0$  is chosen in such a way that  $\beta = 0$  is in the direction of  $(\zeta_1, \zeta_2, 0)$ . That is  $\beta_0 = \theta + \alpha$ . Then,

$$|\zeta_{i*} - \zeta_i| = [P^2 + (w_* - w)^2]^{1/2}. \quad (30)$$

Using Eqs. (29) and (30) in Eq. (25), we have

$$\tilde{L}_1(\phi_J) = \int_0^\infty \int_0^{2\pi} \int_{-\infty}^\infty \Omega_1(\eta, w, P, \beta, w_*) \phi_J(r, \eta_*(\eta, P, \beta), \alpha_*(\eta, \alpha, P, \beta), w_*) dw_* d\beta dP, \quad (31)$$

$$\Omega_1(\eta, w, P, \beta, w_*) = \frac{1}{\sqrt{2\pi}} \frac{P}{[P^2 + (w_* - w)^2]^{1/2}} \times \exp\left(-\frac{(P^2 + 2\eta P \cos \beta + w_*^2 - w^2)^2}{4[P^2 + (w_* - w)^2]} - \frac{P^2 + (w_* - w)^2}{4}\right), \quad (32)$$

$$\eta_*(\eta, P, \beta) = (P^2 + \eta^2 + 2\eta P \cos \beta)^{1/2}, \quad (33)$$

$$\alpha_*(\eta, \alpha, P, \beta) = \alpha + \cos^{-1}\left(\frac{\eta + P \cos \beta}{(P^2 + \eta^2 + 2P\eta \cos \beta)^{1/2}}\right) \quad \text{for } 0 < \beta < \pi, \quad (34)$$

$$\alpha_*(\eta, \alpha, P, \beta) = 2\pi + \alpha - \cos^{-1}\left(\frac{\eta + P \cos \beta}{(P^2 + \eta^2 + 2P\eta \cos \beta)^{1/2}}\right) \quad \text{for } \pi < \beta < 2\pi. \quad (35)$$

Here,  $\eta_* \cos(\alpha_* - \alpha) = \eta + P \cos \beta$  and  $\eta_* \sin(\alpha_* - \alpha) = P \sin \beta$ . Thus,  $0 < \alpha_* - \alpha < \pi$  corresponds to  $0 < \beta < \pi$  and  $\pi < \alpha_* - \alpha < 2\pi$  corresponds to  $\pi < \beta < 2\pi$ . That is why we obtain equations (34) and (35).

The threefold integrals (31) and (26) are computed numerically by first applying the DE transformation and using the trapezoidal formula for the transformed variables.

## References

- [1] C. Cercignani and F. Sernagiotto, "Cylindrical Poiseuille flow of a rarefied gas", *Phys. Fluids* **9**, 40–44 (1966).
- [2] C. -C. Chen, I. -K. Chen, T. -P. Liu and Y. Sone, "Thermal transpiration for the linearized Boltzmann equation", *Commun. Pure Appl. Math.* **60**, 0147–0163 (2007).
- [3] T. Doi, "Numerical analysis of the Poiseuille flow and the thermal transpiration of a rarefied gas through a pipe with a rectangular cross section based on the linearized Boltzmann equation for a hard sphere molecular gas", *J. Vac. Sci. Technol. A* **28**, 603–612 (2010).
- [4] H. Grad, "Asymptotic theory of the Boltzmann equation, II", In *Rarefied Gas Dynamics*(ed. J.A.Laurmann), vol I, pp.26–59 (1963).

- [5] S.K. Loyalka, “Thermal transpiration in a cylindrical tube”, *Phys. Fluids* **12**, 2301–2305 (1969).
- [6] S.K. Loyalka and S.A. Hamoodi, “Poiseuille flow of a rarefied gas in a cylindrical tube: Solution of linearized Boltzmann equation”, *Phys. Fluids A* **2**, 2061–2065 (1990).
- [7] G.A. Radtke, N.G. Hadjiconstantinou and W. Wagner, “Low-noise Monte Carlo simulation of the variable hard sphere gas”, *Phys. Fluids* **23** (2011).
- [8] C.E. Siewert, “Poiseuille and thermal-creep flow in a cylindrical tube”, *J. Comp. Phys.* **160**, 470–480 (2000).
- [9] Y. Sone, *Molecular Gas Dynamics*, Birkhäuser, (2007).
- [10] Y. Sone, T. Ohwada and K. Aoki, “Temperature jump and Knudsen layer in a rarefied gas over a plane wall: Numerical analysis of the linearized Boltzmann equation for hard-sphere molecules”, *Phys. Fluids A* **1**, (1989).
- [11] S. Takata and H. Funagane, “Poiseuille and thermal transpiration flows of a highly rarefied gas: over-concentration in the velocity distribution function”, *J. Fluid Mech.* **669**, (2011).
- [12] H. Takahasi and M. Mori, “Double exponential formulas for numerical integration”, *Publ. RIMS Kyoto Univ.* **9**, 721–741 (1974).